

RESEARCH

Open Access



Study on Reduction Effect of Vibration Propagation due to Internal Explosion Using Composite Materials

Sangwoo Park, Jangwoon Beak, Kukjoo Kim and Young-Jun Park*

Abstract

With the increasing installation cases of underground explosive facilities (e.g., ammunition magazines, hydrogen tanks, etc.) in urban areas in recent years, the risk of internal explosions is also increasing. However, few studies on the measures for reducing damage by the ground vibration have been conducted except for maintaining safety distance. In this study, a method for attenuating the vibration propagated outward by installing a blast-proof panel was numerically and experimentally investigated. Two cubical reinforced concrete structures were manufactured according to the concrete strength and a blast-proof panel was installed on only one side of the structure. Then, acceleration sensors were installed on the external surface to evaluate the propagation of vibration outward depending on the installation of a blast-proof panel. Before a field experiment, a preliminary numerical simulation was performed. The results showed that the acceleration propagated outward could be effectively reduced by installing a blast-proof panel. Even though the performance of a blast-proof panel on vibration reduction was also investigated in the field experiment, significantly larger absolute accelerations were estimated due to the different experimental conditions. Finally, the vibration reduction effect of the blast-proof panel was numerically evaluated according to its thickness and the internal explosion load. A blast-proof panel more effectively reduced the acceleration propagated outward as its thickness increased and the explosion load decreased.

Keywords: internal explosion, blast-proof panel, explosion experiment, safety distance, numerical explosion model

1 Highlights

- A field experiment was carried out to reduce the vibration of a structure by installing a blast-proof panel inside.
- A numerical analysis model was developed to examine the performance of a blast-proof panel on vibration reduction.
- The performance of a blast-proof panel on vibration reduction was investigated depending on various parameters.

2 Introduction

The most effective means for preventing casualties and property damage due to explosions is to adopt blast-proof designs using various structures. Blast-proof design techniques have been developed for military applications, but the demand for such technologies has been rising in the private sector as the risk of explosion in private facilities increases with industrial development. In the private sector, explosions frequently occur in the explosives manufacturing industry, petrochemical industry, and explosive transport vehicles, and are employed intentionally for tunnel excavation or in mines (Due-Hansen & Dullum, 2017). The explosions may lead to significant damages when they occur internally or when dust and explosive agents are present in the air (Abbasi & Abbasi, 2007). In particular, explosions or terrorist attacks in underground

*Correspondence: parky@mnd.go.kr
Department of Civil Engineering and Environmental Sciences, Korea
Military Academy, Seoul 01805, South Korea
Journal information: ISSN 1976-0485 / eISSN 2234-1315

facilities can lead to a large number of casualties; thus, the installation of blast-proof structures or shelters at underground public facilities is essential (Zhang & Wang, 2019).

When dynamic loads are applied to structures, especially reinforced concrete structures, damage caused by cracks and vibrations must be prevented (Golewski, 2019a). In the case of vibration, an appropriate protection method should be applied to prevent the occurrence of harmful vibration or resonance (Golewski, 2021a). Accordingly, research has been conducted to increase the damping performance of concrete by increasing the water ratio and adding mineral and chemical mixture (Golewski, 2019b). The addition of rubberized particles was also attempted to reduce the negative impact of vibrations on concrete structures. Zheng et al. performed free vibration tests for a simply supported beam with rubberized concrete that contains rubber particles (Zheng et al., 2008). The test results showed that the damping ratios of rubberized concrete increased considerably with the increase of rubber contents, indicating the addition of the rubber can decrease the vibration on concrete structures. For cracks, a research result showed that the reduction of microcracks can be expected by injecting an appropriate amount of fly ash (Golewski, 2021b). However, the studies on explosive load, which has a relatively large dynamic load and a short duration, are not actively performed due to the difficulty and danger of the experiment.

The current blast-proof technologies are largely focused on protection structures that protect overpressures, such as blast-proof doors or protective walls. Notably, numerous numerical analysis methods that can predict the structural behavior of a blast-proof door and propagation of explosion pressure have been developed based on the results of periodical qualification tests for blast-proof doors. Lee and Choi simulated overpressures propagated within a blast-proof door using finite element analysis (Lee & Choi, 2018). Choi et al. analyzed the structural behavior of a blast-proof door using the Lagrangian and arbitrary Lagrangian–Eulerian methods. Then, they proposed a more appropriate numerical method according to the configuration of a blast-proof door by comparing the results with those of a field test (Choi et al., 2016). In addition to numerical analyses, studies on welding or structural developments for a blast-proof door have also been conducted to improve the blast-proof performance (Qiang et al., 2020). For protective walls, a large number of studies have been conducted on the blast-proof performance of reinforced concrete. Ruggiero et al. conducted an experiment on contact explosion, which inflicts major local damages under which the behavior of structures is difficult to predict, and developed a numerical analysis

model (Ruggiero et al., 2019). In recent years, studies have been most actively conducted on high-strength concrete for blast-proof structures (Choi et al., 2014; Kunieda & Rokugo, 2006; Yoo et al., 2017). Jung et al. developed high-performance fiber-reinforced cementitious composite (HPFRCC) based on slurry-infiltrated concrete and conducted an in situ explosion experiment. The test results showed that general concrete structures were completely destroyed, whereas HPFRCC did not exhibit damage as the energy of the explosion is consumed due to its increased tensile strength and ductility (Jung et al., 2017). Note that, there is a lack of research on design methods as most studies on reinforced concrete focus on improving the performance of the constitutive materials. The most reliable and generalized blast-proof design involves using unified facilities criteria (UFC) (U.S. 2008). However, it only provides design methods for general concrete. In the case of high-strength concrete with reduced ductility, the use of UFC may lead to additional damage due to tripping of the entire structure or excessive vibration. Therefore, research should be conducted on design techniques for the entire structure along with the improvement of the blast-proof performance of materials.

As such, research on techniques for protection against external loads is mostly focused on the design of blast-proof doors and improvement of material performance, while the consideration of internal explosion has been neglected due to the low probability of its occurrence. However, in recent years, the risk of the internal explosion has been increasing. For instance, large explosions of ammunition magazines in Kazakhstan and Russia caused extensive damages. However, in recent years, the risk of the internal explosion has been increasing. For instance, large explosions of ammunition magazines in Kazakhstan and Russia caused extensive damages to the private sector. Military facilities with the potential risk of explosion are typically located in the outskirts of a city to be separated from highly populated regions. However, cities are becoming larger with accelerated urbanization, which has caused more military facilities to be located in urban areas (Park & Park, 2020). Furthermore, with growing interests in and rapid advancement of technology related to hydrogen energy, facilities with the potential risk of explosions such as hydrogen tanks, hydrogen stations, and hydrogen fuel pipes are expected to be located in urban areas as well (Moradfi & Groth, 2019). In 2019, an explosion due to oxygen inflow and static electricity occurred in Gangneung, Korea, resulting in eight casualties. Accordingly, basic studies have been conducted to analyze the damage patterns through simulations of gas explosions according to ingredients of the gas (Baek et al., 2016; Zhang et al., 2020) and to estimate the extent

of damage to the surrounding environment during explosions (Pyo & Lim, 2019).

During internal explosions, the explosion pressure is irregularly reflected due to partially or fully confined structures, which overlap each other to generate a maximum overpressure higher than the external explosion. Moreover, a relatively long time is required for the overpressure to decrease due to insufficient space for the pressure to escape. Therefore, the explosion impulse applied to structures and facilities further increases. In addition, the purpose of protection is different from that in the case of external explosions: in the case of external explosions, it is to protect the subjects (persons, properties, other explosives, etc.) against the explosion pressure or fragments, whereas for internal explosions it is to prevent the facility from collapsing and to minimize propagation to outside. Accordingly, research on internal explosions mostly focuses on predicting the changes in explosion pressure within a facility caused by explosions. A boiling liquid expanding vapor explosion (BLEVE) is a type of explosion caused by compressed gas, such as liquefied petroleum gas (LPG), exploding within a vessel. When explosives are transported on a vehicle (e.g., LPG road tanker accidents), BLEVE can occur inside a tunnel in which gas expansion is not sufficient, and the explosion wave slowly dissipates, due to the long and narrow structure of a tunnel, resulting in heavy damages to the facility and people inside it (Masellis, 2000). Genova et al. proposed an empirical formula for predicting the explosion pressure and the initial speed of fragments of BLEVE (Genova et al., 2008); Silvestrini et al. predicted the internal explosion pressure of BLEVE by applying the concept of energy concentration factor (ECF) (Silvestrini et al., 2009). ECF is a predictive model for predicting the overpressure of the blast wave; thus, it can predict even the explosion pressure in an underground network of a platform to a certain extent in addition to external explosions. Numerous studies have also been conducted on predicting the changes in pressure during internal explosions through numerical analyses. Uystepuyst et al. developed and verified a numerical model for the changes in explosion pressure inside a rectangular tunnel (Uystepuyst & Monnoyer, 2015). Zhang et al. used the ANSYS/LS-DYNA program to create a numerical model for designing a shelter within a coal mine and calculated the pressure and stress according to the shelter structure (Zhang et al., 2014).

Furthermore, studies on designs for attenuating the explosion pressure propagating outside during internal explosions have been increasing (Igra et al., 2013). Sklavounos and Rigas analyzed the effect of vents inside a tunnel on pressure attenuation based on numerical analysis. The attenuation effect increased as the number

of vents and their diameters increased, whereas the angle of the vent did not have a significant effect (Sklavounos & Rigas, 2006). Zhang et al. analyzed explosion pressure propagation according to the number and angle of branch galleries inside a tunnel through computational fluid dynamics (CFD) analysis. The results showed that the pressure of the main pathway decreased as the angle of a branch gallery increased (Zhang et al., 2013). In addition, experiments and numerical analyses were performed to reduce the released explosion pressure by installing mixed water and sand inside an underground ammunition facility (Homae et al., 2016; Sugiyama et al., 2016). However, it is impractical that installing multiple vents, branch galleries, a mixed material of water and sand in actual facilities. The blast-proof panel has also been developed that reduce the explosion pressure by allowing inelastic deformation using stainless steel with high ductility property (Langdon & Schleyer, 2005a). For the developed blast-proof panel, a theoretical approach and numerical analysis were performed for estimating displacement (Langdon & Schleyer, 2005b, 2006). One of the solutions for mitigating vibration in concrete structures is to use periodic rubber concrete panels. Chen and Shi carried out parametric studies on different geometric periodic panels (Bragg-scattering and Local-resonant periodic panels) and concluded that the vibration can be reduced significantly by using a periodic structure with only three units (Cheng & Shi, 2014). However, these theoretical results were not yet backed up by the actual experimental tests.

Recent studies on internal explosion mainly involve experiments conducted in a laboratory and numerical analysis; field tests are rarely conducted due to safety risks and limitations of cost and appropriate sites to form mock-up facilities. In particular, internal explosions occurring in underground facilities may cause vibration propagation through the ground, besides pressure propagation through openings, which may damage nearby facilities. Ground vibration may lead to a reduction in stability and usability of nearby facilities on or below the ground, and cracking or destruction of structures may occur due to relative displacements to the ground formation. Thus, the safe distance is determined based on the vibration acceleration of ground particles when designing an underground ammunition storage facility (Department of Defense, 2017; Ministry of National Defense, 2019; Organization et al., 2015). The safe distance refers to the minimum distance required for protecting lives and property from explosion pressure, fragments, debris, and ground vibration in the case of accidental explosions of an ammunition storage facility. The safety of ground vibration should also be considered as the subject of inspection because the demand for

construction of hazardous facilities on explosion such as underground roads or underground storage facilities increased in urban areas. In addition, military facilities including ammunition storage magazines and bunkers are built underground due to military reform measures for civil–military coexistence. However, few studies have been conducted on design plans or techniques to reduce the ground vibration. Existing blast-proof panels can be ineffective as a method of reducing the ground vibrations propagating to the outside in response to internal explosions because they allow excessive deformation to decrease explosion pressure.

Increasing the thickness of concrete is a common means for reducing the ground vibration being propagated outward from the explosion in underground facilities. However, this method is difficult to apply to underground facilities, is quite expensive, and may cause negative environmental impacts, such as CO₂ emission during curing and mixing. Therefore, in this study, a method for attenuating the vibration propagated outward by installing a blast-proof panel consist of composite materials of special structural steel, aramid fiber, and foam material was considered. This study aims to reduce vibration as much as possible by installing blast-proof panels to reduce the safety distance of underground facilities with the possibility of explosion. First, to experimentally analyze the vibration reduction effect, structures were manufactured with reinforced concrete, and blast-proof panels were attached on one side of the wall. Two reinforced concrete structural bodies were manufactured, one with normal strength and one with high strength, to evaluate the performance of the blast-proof panel depending on the concrete strength. Due to the high risk of explosion and impossibility of repeating the experiment after the structure is destroyed, a preliminary simulation was conducted using the ANSYS AUTODYN program to investigate the vibration reduction effect in advance. Based on its results, trinitrotoluene (TNT) with a net explosive weight of 5.9 kg was exploded in a completely confined space, and the acceleration propagated to the external wall was measured to determine the vibration reduction effect. Furthermore, the reduction effect of the blast-proof panel depending on panel thicknesses and explosion loads was evaluated with the numerical model used during the preliminary numerical analysis.

3 Experimental Conditions of Field Test

For simulating an internal explosion within a structure, a cubical reinforced concrete structure with a hole was manufactured. The blast-proof panel was composed of high-strength structural steel, aramid fiber, and energy-absorbing foam, for effectively absorbing the blast pressure and collision energy. The blast-proof panel had

500 mm of thickness and secured on the wall using a frame made of high-strength structural steel, as shown in Fig. 1.

The interior of the structure was 1.5 × 1.5 × 1.5 m (width, length, and height, respectively). These dimensions were chosen considering the size of the blast-proof panel (1.5 m in width and 0.75 m in length). The TNT was set to have a net explosive weight of approximately 5.9 kg (= 13 lb), based on a 152-mm shell to be appropriate for the downscaled structures. The thickness of the concrete wall was chosen to be sufficient to prevent cracks as measuring devices attached to the external wall may fall if the structure is destroyed or cracks are generated on the external surface. Based on the technical manual (TM), all four walls are designed to be 0.5 m thick so that only micro-crack damage occurs during the explosion (Army, 1986). Then, the external size of the structure was 2.5 × 1.5 × 2.5 m (width, length, and height, respectively) as shown in Fig. 2a.

As mentioned above, two reinforced concrete structures were manufactured for the experiment, one made of normal strength concrete with a target strength of 24 MPa, and the other made of high-strength concrete with a target strength of 80 MPa. Table 1 presents the mixture design for the normal- and high-strength concretes. Each mix design of fly ash, blast furnace slag, and superplasticizer in the high-strength concrete used for the specimen is not disclosed due to the trade secret of the concrete manufacturer.

The blast-proof panel was attached on only one side of the structure to evaluate the degree of blast-pressure reduction in the presence of the panel based on the acceleration measured on the external wall of the structure after the internal explosion. Since the experiment was conducted with installing blast-proof panels on only one side of the walls, the panels were not installed on both the roof and the floor to induce the same incident pressure

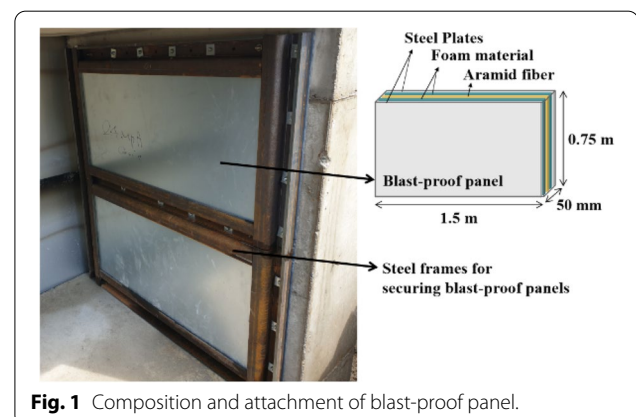


Fig. 1 Composition and attachment of blast-proof panel.

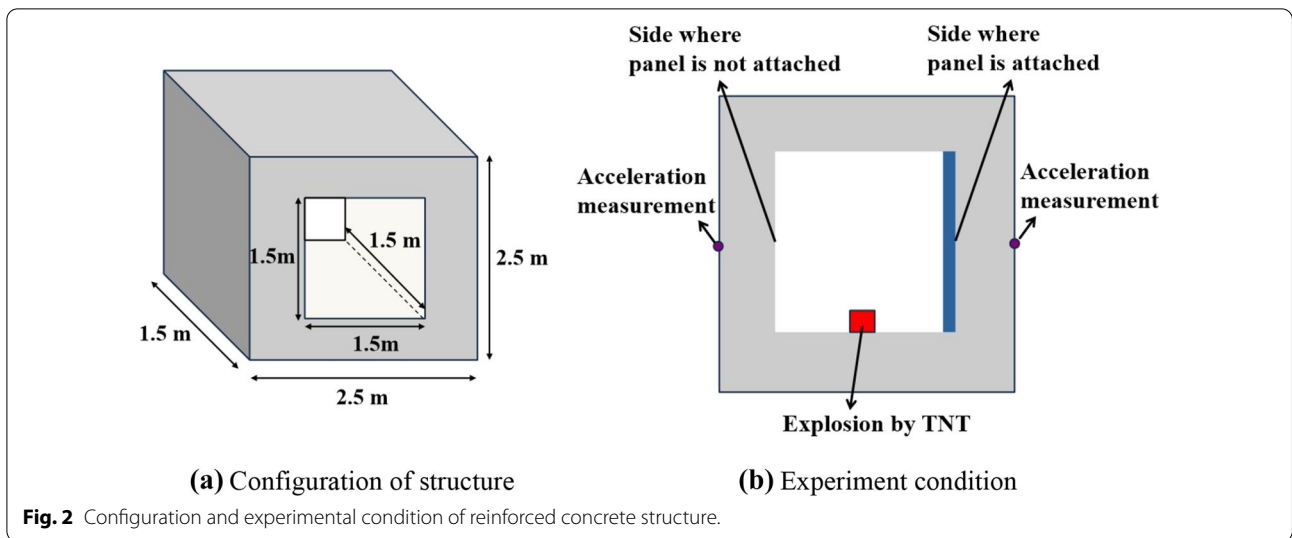
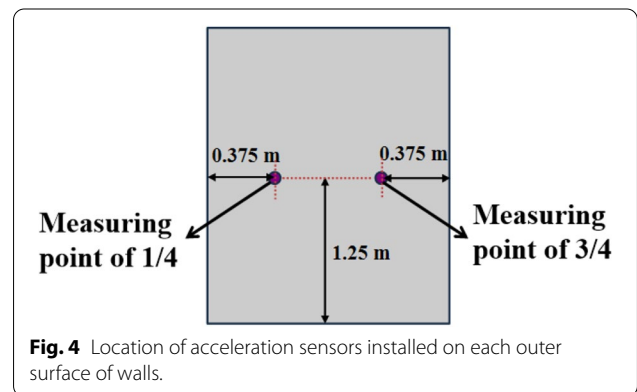
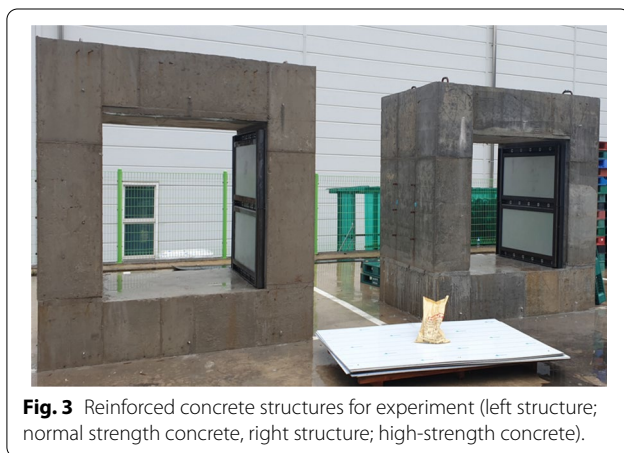


Table 1 Material properties of concrete used in simulation

Target compressive strength (MPa)	W/C (%)	Unit weight, (kgf/m ³)							Slump (mm)	Maximum aggregate size (mm)
		W	C	FA	CA	FS	S	SP		
24	33.3	161	340	749	956	58	85	4.1	120	25
80	11.1	130	1026	1140	1075	114			25	19

W: water; C: cement; FA: fine aggregate; CA: coarse aggregate; FS: fly ash; S: blast furnace slag; SP: superplasticizer, 1 mm = 0.0374, 1 m = 3.281 ft, 1 kgf = 2.204 lbf.



to both walls. Thus, the acceleration was measured on a total of four external walls. Figure 2b shows the experimental conditions inside the structure where the blast-proof panel was installed. Figure 3 shows the structure after manufacturing.

Two acceleration sensors were installed on each surface at the center of the height at 1/4 and 3/4 points in the horizontal direction. The model 3200B by DYTRAN with

a capacity of $\pm 10,000$ g, allowable temperature between -15 and 121°C , and frequency response in the range 0.35–10,000 Hz was used. To prevent the acceleration sensors from falling due to the vibration of structures, they were fixed with jigs to the rebars after placing the reinforcement and before pouring the concrete. After curing the concrete, the acceleration sensors were attached to the jigs buried in the concrete. The location of installed acceleration sensors and process of installing jigs are shown in Figs. 4 and 5, respectively.

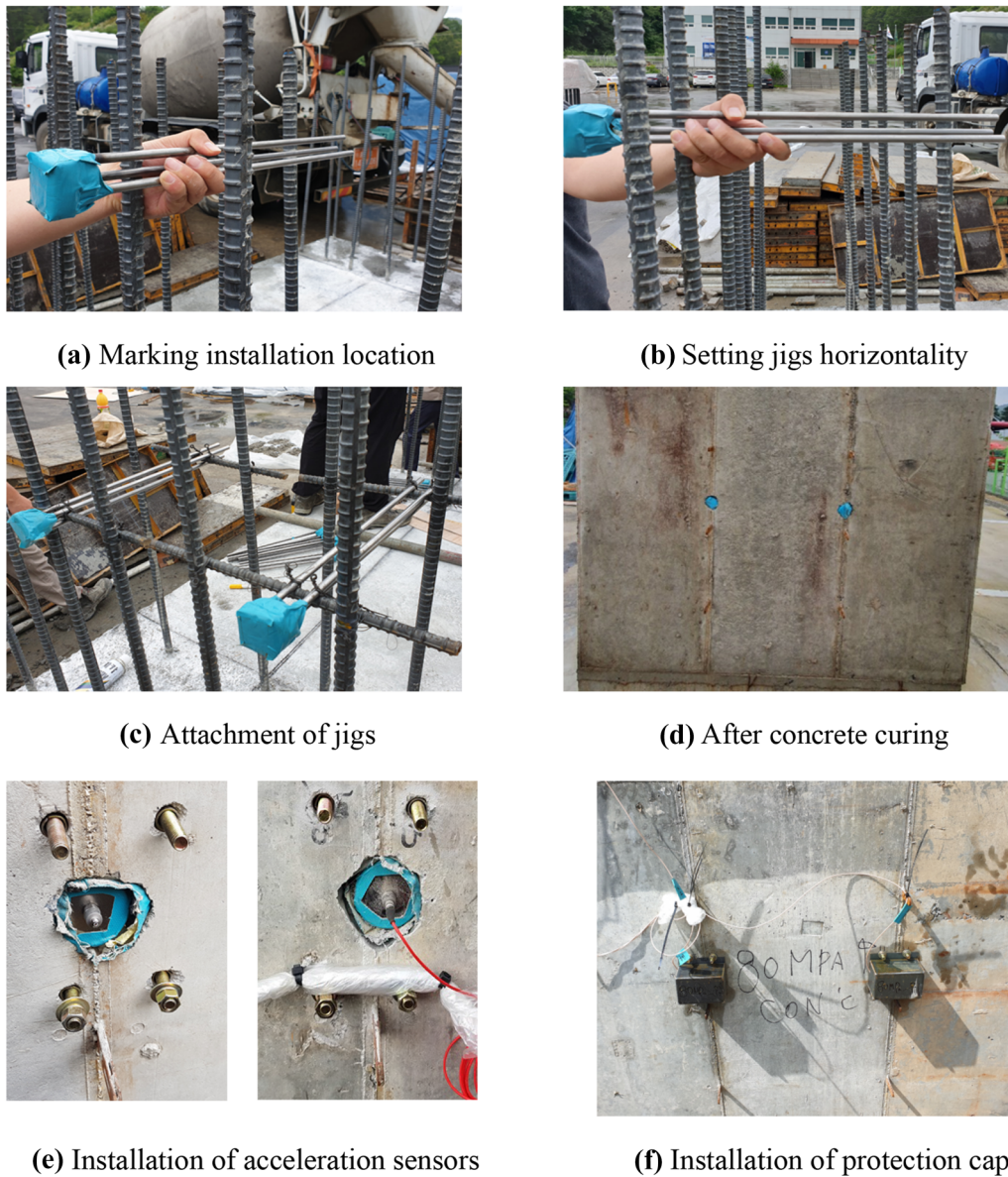


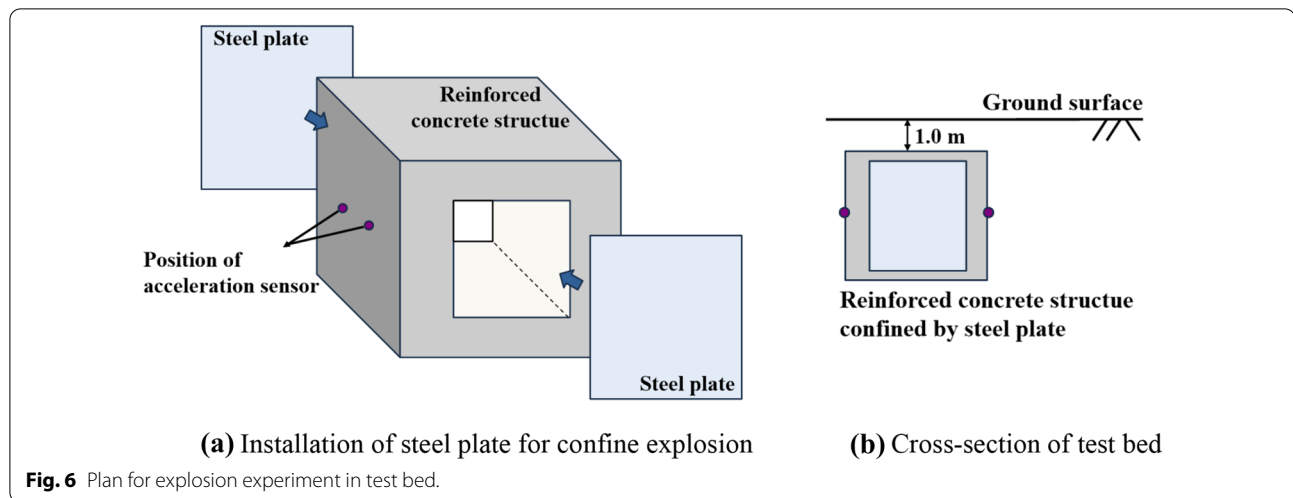
Fig. 5 Installation process of jigs and acceleration sensors.

The rebars in the concrete were placed at the minimum reinforcement ratio. For the normal strength concrete, D16 rebars were placed at intervals of 175 mm, satisfying the reinforcement ratio of 0.306%; for the high-strength concrete, D22 rebars were placed at intervals of 175 mm, satisfying the reinforcement ratio of 0.559%. Moreover, D16 shear rebars were placed at the interval of 175 mm using 90° and 135° cross hooks for resistance in the direction of blast pressure.

Openings were made in the front and back sides of the structures to facilitate the installation of TNT by reducing the risk and enabling the TNT ignition lines to be

taken outside. However, as the explosion has to occur in a completely confined space for the experiment, 5-mm steel plates were attached to the openings, and the structures were planned to be buried underground to simulate complete confinement. The two structures were positioned approximately 30 m apart in the test field. Figure 6 illustrates the experiment plan.

In conclusion, two structures, one made of normal strength concrete (target strength of 24 MPa) and the other of high-strength concrete (target strength of 80 MPa), were manufactured. A blast-proof panel was installed on one side of each structure to enable the



analysis of vibration reduction performance depending on the presence of the panel and on the strength of the concrete. The vibration reduction effect was evaluated by measuring the acceleration propagating outward during an internal explosion with acceleration sensors installed on the external wall of the concrete structures. In addition, the structures were planned to be buried underground to simulate an internal explosion within a completely confined structure.

4 Preliminary Numerical Simulation

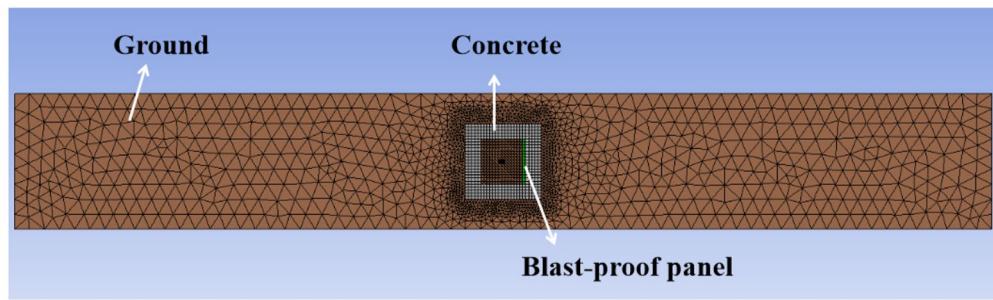
4.1 Development of Numerical Analysis Model

A field experiment for explosions can only be conducted once as the experiment is hazardous and the structure is destroyed. Furthermore, the results may be influenced by various environmental factors on the test day, and uncertainties exist in terms of the performance of the blast-proof panel against an internal explosion under the predetermined experimental conditions. In other words, it was uncertain that the vibration reduction effect can be accurately measured when the blast-proof panel was installed on only one side of a structure. Hence, the ANSYS AUTODYN program was used to perform a preliminary numerical simulation before the actual experiment. ANSYS AUTODYN is a commercial program that can analyze the interaction between a fluid and a structure by modeling the ground and the atmosphere which are the media through which blast pressure travels. Based on the coupled analysis, the blast pressure load and the structure's response can be simultaneously calculated.

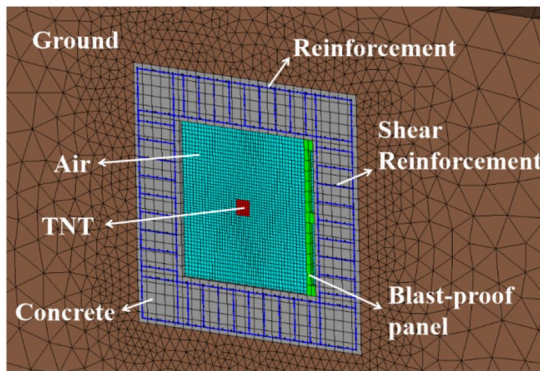
First, the modeling was performed considering the manufactured structure buried 1 m underground. A blast-proof panel is typically made of various composite materials, but it was assumed to be made of one material with equivalent properties to facilitate the analysis. The

explosion load was applied at the same amount as would result from the TNT explosion to be used for the experiment. The reinforcement placement was modeled with the same reinforcement ratio as the manufactured structure. The mesh of concrete, blast-proof panel, and atmospheric layer was composed of hexahedrons, whereas that of the surrounding ground was composed of tetrahedrons. The mesh of air, structure, and blast-proof panel consisted of 174,000, 2400, and 120 meshes, respectively. The contact surface of each structure and ground was composed of a mesh having a size of 100 mm. In the case of the ground, a tetrahedral mesh was configured to gradually increase as it apart from the structure. The structure buried underground and the modeling results of the blast-proof panel are shown in Fig. 7.

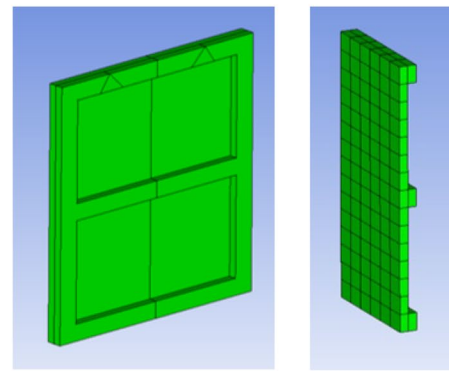
For the concrete material failure model, the Riedel–Hiermaier–Thoma (RHT) dynamic damaged concrete model was applied. This model provides a relationship of failure, elastic limit, and residual behaviors against an explosion load. On the other hand, the Drucker–Prager model, which can simulate the plastic deformation of the soil, was applied to the ground formation. The boundary condition of each material was set to the bonded condition. However, the frictional condition was applied to the boundary between the atmosphere and ground as the 5-mm-thick steel plate installed at the opening is limited for modeling due to the convergence problem. Sliding or separation does not occur in the bonded condition, whereas they may occur in the frictional condition due to shear stress between the boundaries. Moreover, interpenetration that may occur at the contact surface due to the displacement generated by the blast pressure was controlled by contact stiffness using the Lagrange contact formulation in the numerical model. For the material properties of



(a) Overall numerical model



(b) Embedded structure model



(c) Blast-proof panel model

Fig. 7 Modeling result for preliminary numerical simulation.

Table 2 Material properties of concrete used in simulation

Property	Normal strength concrete	High-strength concrete
Density	2304 kg/m ³	2304 kg/m ³
Compressive strength	24 MPa	80 MPa
Tensile strength	2.4 MPa	8 MPa
Shear strength	4.32 MPa	14.4 MPa
Bulk modulus	3.21 × 10 ⁴ MPa	5.52 × 10 ⁴ MPa
Shear modulus	1.48 × 10 ⁴ MPa	2.47 × 10 ⁴ MPa

Table 3 Material properties of ground and blast-proof panel applied in numerical simulation

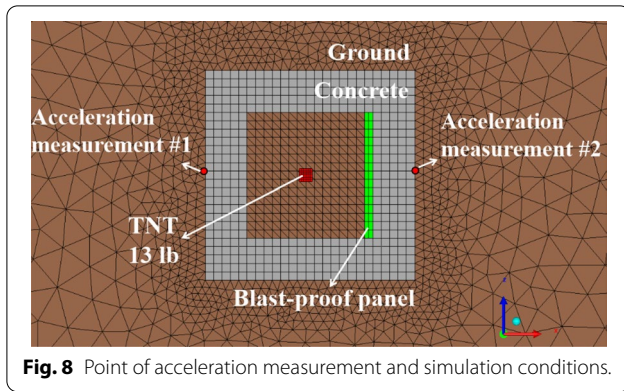
Material	Property	Value
Ground	Density	1920 kg/m ³
	Bulk modulus	2.07 × 10 ⁴ MPa
	Shear modulus	7.85 × 10 ³ MPa
	Poisson's ratio	0.332
Blast-proof panel	Density	0.5 kg/m ³
	Yield stress	2.6 MPa
	Bulk modulus	7.92 × 10 ⁴ MPa
	Shear modulus	3.65 × 10 ⁴ MPa
	Poisson's ratio	0.3

concrete, the experimental values for impact provided by AUTODYN and references were used, as presented in Table 2 (Riedel et al., 2009).

The test bed been was a quarry in the past, and the ground was extremely hard and excavation was difficult. Therefore, the material properties of the ground obtained from the experimental values of hard rock in a nearby site were used in the simulation (Park et al., 2019). The material properties of the ground and blast-proof panel applied in the numerical simulation are presented in Table 3.

4.2 Result of Preliminary Numerical Simulation

The experiment was preliminarily simulated through the developed numerical model. The acceleration was measured at the contact surface between the ground and concrete after inducing the same explosive amount as the field test condition to be exploded. As shown in Fig. 8, the acceleration value was calculated considering the blast-proof panel installed only on one side, and the



vibration reduction effect of attaching the blast-proof panel was evaluated. The simulation results (i.e., changes in the acceleration at the contact surface of concrete and ground according to time) are shown in Fig. 9.

The red and blue lines in Fig. 8 represent the accelerations measured at the external walls where the blast-proof panel was not installed (i.e., position #1) and where the blast-proof panel was installed (i.e., position #2), respectively. The results of a preliminary numerical simulation showed that the acceleration propagated outward from the side with the blast-proof panel is reduced for both structures. In particular, the acceleration peak generated after the first peak is higher at the side with the blast-proof panel installed, which indicates that the blast-proof panel effectively reduces the damage caused by the initial explosion load. To quantitatively analyze the vibration reduction effect of a blast-proof panel, the maximum

acceleration derived by measuring on each surface is summarized in Table 4.

When an internal explosion occurs, the maximum pressure applied to the structure is amplified as the pressure is reflected by the surrounding walls. The degree of pressure amplification due to reflection is determined by explosion load (i.e., net explosive weight, distance with walls, etc.), the volume of the internal space, and the incidence angle of explosion pressure to walls. The degree of pressure amplification due to reflection is not significantly affected by the strength of concrete because there is no significant difference in density. However, the response of the structure by the reflected pressure is greatly influenced by the stiffness of the structure. The response of the structure to the same reflected pressure increases as the ratio of the duration of the explosion load to the natural period of the structure increases. That is, as the stiffness increases, the response of the structure to the reflected pressure increases. Therefore, when the blast-proof panel is not installed, vibration at the outside

Table 4 Vibration reduction effect of blast-proof panel in preliminary numerical simulation

Concrete strength	Maximum acceleration (mm/ms ²)		Reduction effect (%)
	#1 (without panel)	#2 (with panel)	
Normal strength concrete	6.10	4.12	32.46%
High-strength concrete	5.74	3.64	36.59%

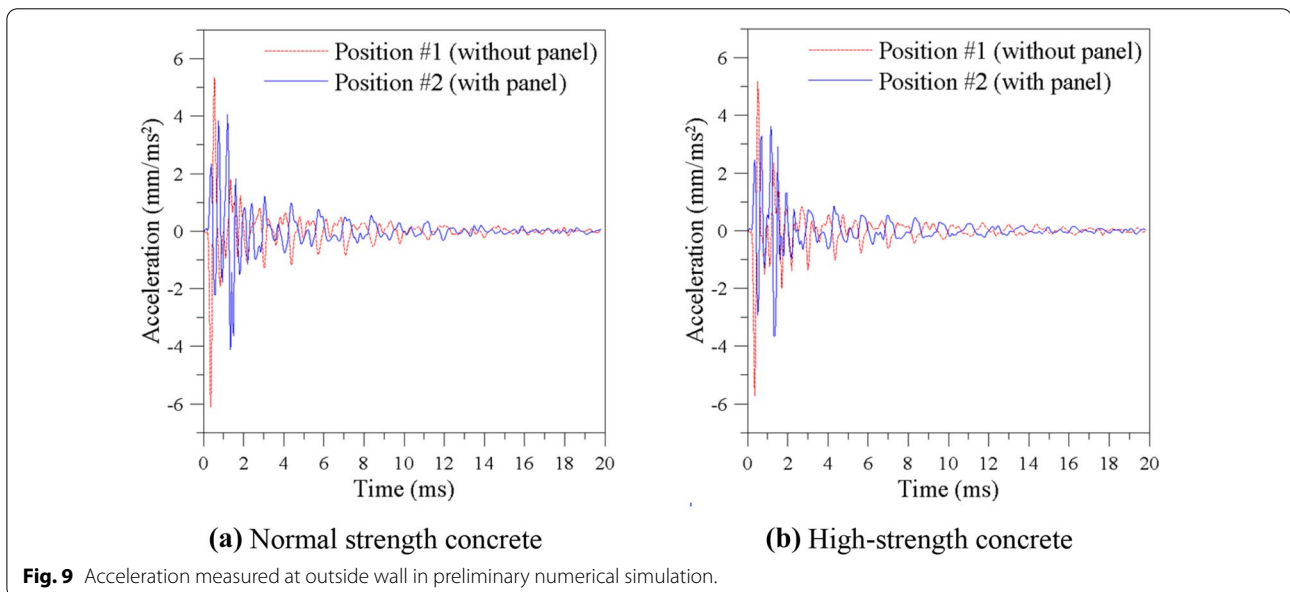


Fig. 9 Acceleration measured at outside wall in preliminary numerical simulation.

wall should be greater in high-strength concrete with high stiffness than normal strength concrete. However, when the structure was surrounded by ground formation with relatively smaller stiffness as the numerical model, the effective stiffness of the entire media decreases. Moreover, the degree of reduction of effective stiffness varies depending on the difference of properties between the structure and surrounding ground. Therefore, as shown in the preliminary numerical analysis result, about 6% greater vibration occurred in the normal strength concrete than in the high-strength concrete when the panel was not installed.

In the same way, when materials with relatively smaller stiffness such as blast-proof panels were attached, the degree of reduction in stiffness of high-strength concrete was greater than normal strength concrete. Therefore, the reduction effects in normal and high-strength concretes were 32.46% and 36.59%, respectively, indicating that the vibration reduction effect is more pronounced in the structure made of high-strength concrete.

Under the conditions of the preliminary numerical analysis, the incident pressure (i.e., explosion pressure before reflection) can be predicted to be about 50 kg/cm² according to the TM (Army, 1986). In contrast, the maximum reflected pressure is estimated to be about 385 kg/cm² in the internal explosion, which is 7.7 times higher than incident pressure. Furthermore, in an internal explosion, the load duration is increased compared to the external explosion because the pressure is continuously reflected, and is not efficiently discharged to the outside. Eventually, the amount of impact the structure receives becomes considerably larger than external explosion. In other words, not only the danger of the structure itself where the explosion occurred, but also the possibility of damage to the surrounding facilities significantly increases when the internal explosion occurs. Therefore, installing blast-proof panels on structures with high

potential for internal explosion may be a very important and effective design method for safety.

In summary, installing a blast-proof panel reduced the vibration propagated outward due to an internal explosion in an underground facility by approximately 34.53% according to the preliminary simulation results. A higher acceleration was measured in normal concrete at the measuring point where the blast-proof panel was not installed (i.e., position #1), and the vibration reduction effect due to the installation of a blast-proof panel was higher in high-strength concrete. For experimental verification, an in situ explosion experiment was performed at the test bed.

5 In Situ Explosion Experiment

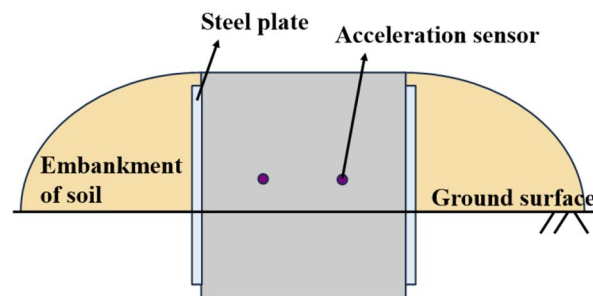
5.1 Compositions of Test Bed and Experiment

The experimental structures were transported from the curing site to the experiment site on a truck. The excavation was performed in advance and the structures were carried to the experiment location using a crane. Similar to the preliminary numerical simulation, the concrete structures were planned to be buried underground at 1 m deep for the experiment. However, due to heavy rain on the day of the experiment, burying was impossible as the ground was filled with groundwater (Fig. 10a). Thus, the ground was excavated 1 m deep to place the structures instead, as shown in Fig. 10b. After confining the opening with 5-mm-thick steel plates, the surrounding soil was piled up to fixate the steel plates as much as possible. Figure 11 shows the structures before the experiment.

The blast test was performed two times. In the first experiment, the explosion was carried out for the normal strength concrete structure. After confirming the stabilization of fragments and the ground vibration, the second explosion was performed for the high-strength concrete structure. Figure 12 shows the field explosions of the normal and high-strength concrete structures.



(a) Field condition



(b) Cross-section of changed test bed

Fig. 10 Changed experimental conditions due to field condition on experiment day.



(a) Normal strength concrete structure before explosion



(b) High-strength concrete structure before explosion

Fig. 11 After installation of experimental reinforced concrete structures.



(a) Normal strength structure



(b) High-strength structure

Fig. 12 Energy and fragment emission during explosion experiment.

As shown in Fig. 12, the fragments scattered farther in the normal strength structure, whereas the internal explosion energy was relatively more concentrated in the high-strength structure. It can be inferred that the roof slab of the normal strength structure was destroyed and separated due to the blast pressure, as shown in Fig. 13a.

The displacement of the structure due to the reflected pressure is greatly affected by the strength of the structure. The larger the explosion load compared to the strength of the structure, the greater the displacement of the structure will occur. That is, in the normal strength concrete structure, the displacement of each member occurred larger, and the reinforcement ratio was also less than in the high-strength concrete structure. Therefore, the failure of the upper slab, which had a small external binding force than other members, occurred. In contrast, diagonal and transverse tension cracks were found in the high-strength structure, but the structure did not collapse. The blast-proof panels can reduce the reflected

pressure due to internal explosion by absorbing the explosion load, but the reduction ratio may be similar in the two structures.

Moreover, the explosion pressure was released in all four directions for the normal strength structure due to the structure destruction. On the other hand, since the high-strength structure maintained its initial form after the explosion, the confining pressure was maintained, so it can be estimated that the internal explosion energy was higher than in the normal strength structure.

5.2 Analysis of Experimental Data

The experimental results (i.e., changes in the acceleration at the external concrete wall according to time) are presented in Fig. 14. In addition, the maximum acceleration measured from each surface and the vibration reduction effect according to the installation of a blast-proof panel are summarized in Table 5. #1 and #2 in Fig. 14 and Table 5 refer to the external wall without and with the



(a) Normal strength concrete



(b) High-strength concrete

Fig. 13 Experimental structures after blast test.

panel, respectively, as in the preliminary numerical simulation. Furthermore, 1/4 and 3/4 refer to the measuring point of 1/4 and 3/4 locations in a horizontal direction at which two acceleration sensors were attached on the external wall for the experiment.

The in situ explosion experiment results revealed that the acceleration propagated to the external wall during an internal explosion was significantly reduced by installing a blast-proof panel. In addition, similar to the results of the preliminary numerical simulation, the peak value occurred relatively later (i.e., after the first peak value) when the blast-proof panel was installed. In other words, the blast-proof panel effectively reduced the damage caused by the initial explosion load. However, the structures were not completely confined due to rain, and the upper slab of the normal strength structure was destroyed after the explosion, which resulted in a significant difference in the acceleration values measured at 1/4 and 3/4 points on the wall of the normal strength structure at which the blast-proof panel was not installed. The acceleration reduction effect by the blast-proof panel could not be clearly identified at the 3/4 point in the normal strength structure. Therefore, the reduction effect of the blast-proof panel in Table 5 was calculated based on the maximum acceleration measured from each surface. The calculation results showed that the reduction effects in normal and high-strength structures were 28.87% and 45.13%, respectively. Meanwhile, Table 6 presents the comparison of the numerical simulation and in situ explosion experiment results.

The acceleration values measured during the field test were significantly higher than the values obtained from the preliminary numerical simulation. The following three reasons can be inferred. First, the structures

were buried underground to completely confine the surrounding with the ground formation in the preliminary numerical simulation, whereas the structures were exposed to the air during the in situ explosion experiment. Thus, a larger vibration occurred as the confinement by a surrounding medium was removed during the in situ explosion experiment. Second, the 5-mm-thick steel plates and soil completely blocked the opening and the TNT exploded at the bottom of the structure during the in situ explosion experiment. That is, an internal explosion occurred in a completely confined state, and the TNT exploded from the bottom surface, which maximized the increase of the explosion pressure due to the reflective pressure initially generated. In general, the pressure increases more substantially when the explosion occurs while in contact with the ground surface (or floor) when compared to the explosion occurring in mid-air (U.S., 2008). Contrarily, the explosion occurred in mid-air and the surrounding steel plates were not modeled in the preliminary numerical simulation, which resulted in the increase of the pressure from an internal explosion being relatively smaller. Finally, the jigs that were fixated by connecting with the reinforcing structural steel during concrete curing were used in the in situ experiment, as shown in Fig. 3, to install the wall's acceleration sensors. Therefore, the vibration of the structural steel from the internal explosion may have significantly affected the measured acceleration.

In addition, the acceleration measured on the external wall without the blast-proof panel was larger in the high-strength structure, unlike the results of the preliminary numerical simulation. The explosive pressure was quickly released to the outside as the upper slab of the normal strength structure collapsed due to the

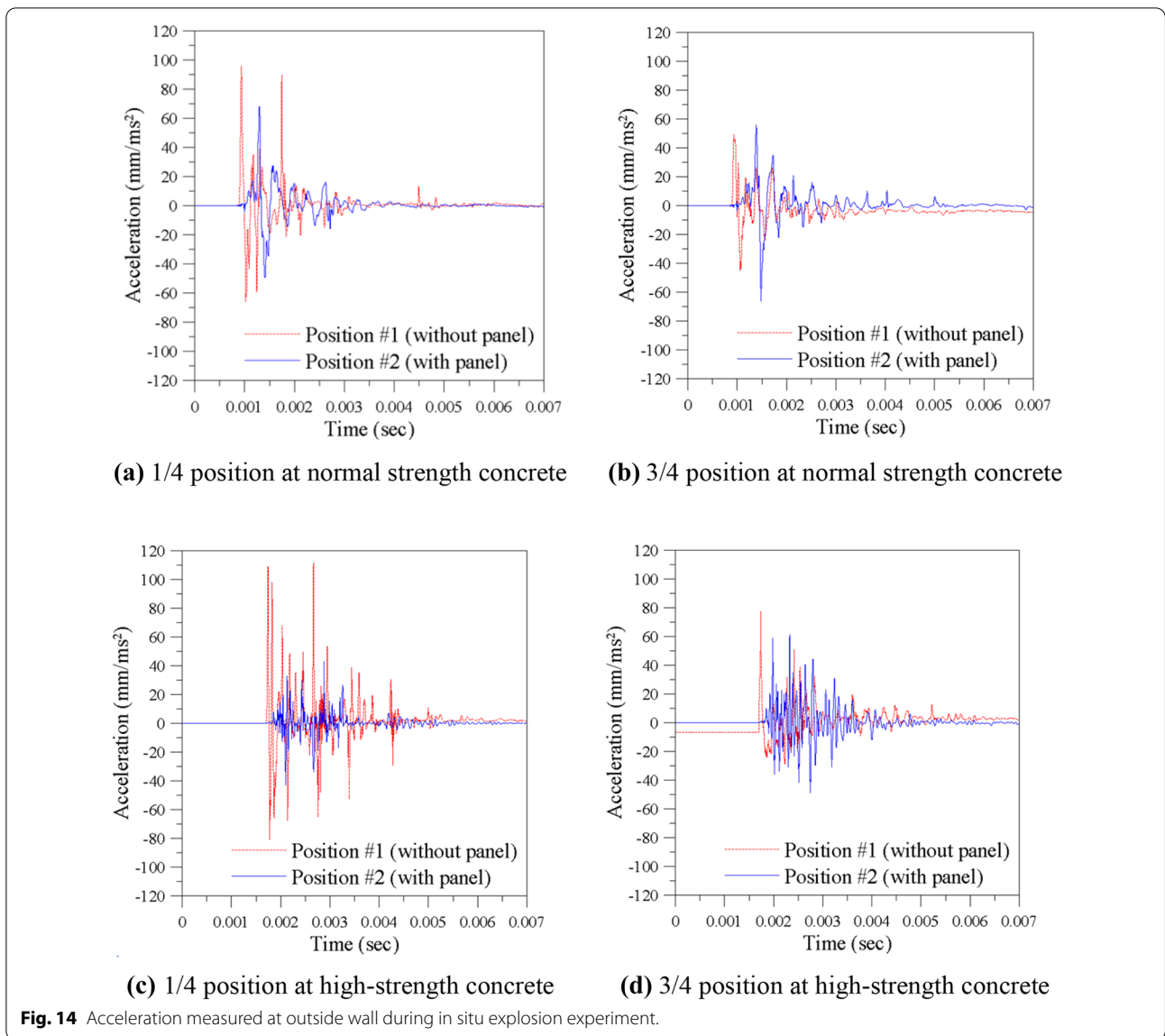


Table 5 Vibration reduction effect of blast-proof panel in field experiment

Concrete strength	Maximum acceleration (mm/ms ²)		Reduction effect (%)
	#1 (without panel)	#2 (with panel)	
Normal strength concrete			
1/4	95.82*	68.16*	28.87%
3/4	49.21	66.62	
High-strength concrete			
1/4	111.79*	42.88	45.13%
3/4	84.34	61.33*	

* Maximum value among measured at point 1/4 and point 3/4.

explosion. As mentioned above, the pressure amplifies as the explosion pressure is irregularly reflected on the walls in all four directions during an internal explosion. As the amplified pressure cannot be easily released to the outside, the impact against the walls increases more (U.S., 2008). However, in this experiment, the reflective pressure was relatively smaller due to the destruction of the normal strength structure, and a small impact was applied to the walls as the blast pressure was easily released to the outside compared to the high-strength structure.

Due to various restrictions at the field, the absolute value of the acceleration measured during the field test varied significantly from the results of the preliminary numerical simulation. However, the vibration reduction

Table 6 Comparison of numerical simulation and field experiment results

Experiment	Concrete strength	Maximum acceleration (mm/ms ²)		Reduction effect (%)
		#1	#2	
Numerical simulation	Normal strength	6.10	4.12	32.46%
	High-strength	5.74	3.64	36.59%
Field test	Normal strength	95.82	68.16	28.87%
	High-strength	111.79	61.33	45.13%

#1: Outside surface of concrete on the side without blast-proof panel.

#2: Outside surface of concrete on the side with blast-proof panel.

effect of installing a blast-proof panel was similar in both cases. Furthermore, the reduction effect was superior in the high-strength structure in both the preliminary numerical simulation and the field test due to the difference in material properties from the surrounding medium, as explained. In addition, the confining points of walls by the upper slab was eliminated as the upper slab of the normal strength structure was destroyed, which caused an additional vibration and resulted in the lowered vibration reduction effect by the panel.

6 Parametric Analysis Through Preliminary Numerical Model

A parametric analysis was conducted using the preliminary numerical simulation model, and the vibration reduction effect was deduced according to the blast load and the thickness of the blast-proof panel. The standard blast load was set based on the condition used in the preliminary numerical simulation (i.e., TNT with a net explosive weight of 5.9 kg). Then, the numerical simulation was performed by changing the net explosive weight of TNT from 2.95 to 11.8 kg and 47.2 kg. Similarly, the standard thickness of the blast-proof panel was set based on the condition used in the preliminary numerical simulation (i.e., 50 mm thickness), and the numerical simulation was performed by changing the thickness from 25 mm to 100 mm and 200 mm. The other conditions were maintained. The variables considered in this study are summarized in Table 7.

The simulation results under varying blast loads are shown in Figs. 15 and 16 according to concrete strength. And, the maximum acceleration at each measuring point is summarized in Table 8.

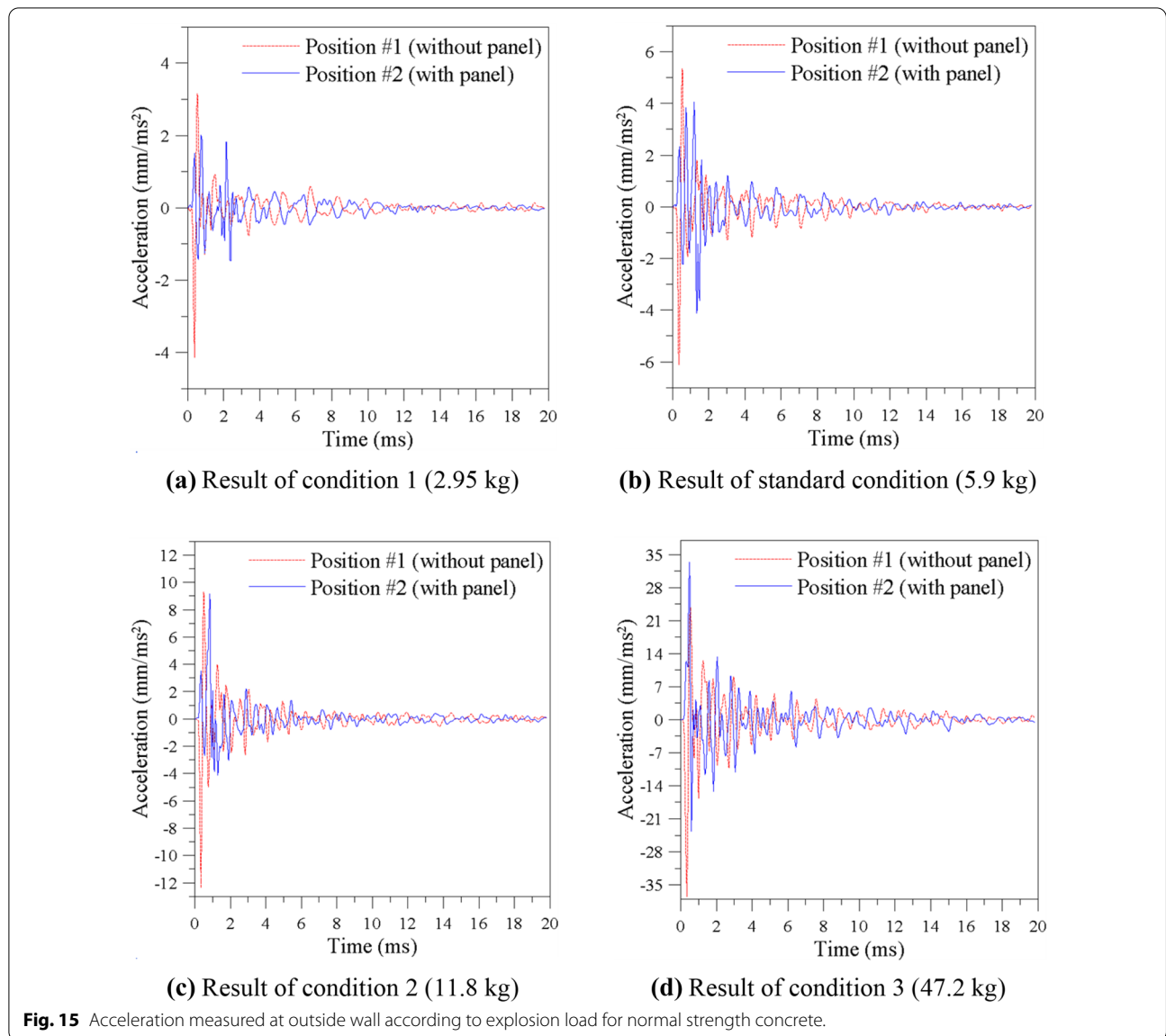
Similar to the results of the preliminary numerical simulation, the acceleration reduction effect at the external wall due to the installation of the blast-proof panel was smaller in normal strength concrete. The increased accelerations were clearly exhibited at all walls as the explosion load increased. The pressure amplified by reflection on the walls in all four directions was exponentially increased as the explosion load increased (U.S., 2008). Moreover, as the explosion load increased, the reduction effect on the acceleration propagated outward by installing a blast-proof panel gradually decreased. The vibration transmitted through the structure itself increased as the explosion load increased. Also, the tremor of the materials on the side at which the panel was installed could not be effectively prevented due to cracks in the structure. The degree to which the acceleration reduction effect is lowered due to an increased explosion load is similar in both normal- and high-strength structures.

The simulation results according to the thickness of a blast-proof panel are shown in Figs. 17 and 18. And, the maximum acceleration at each measuring point is summarized in Table 9.

The acceleration reduction effect of installing a blast-proof panel was higher in the high-strength structure, likewise previous analysis results. The acceleration propagated outward was more effectively reduced as the thickness increased. However, the increasing rate of the thickness was not proportional to the acceleration reduction effect, which implies that the optimal thickness should be selected by considering economic feasibility and constructability.

Table 7 Variables considered in parametric study

Parameters	Condition 1	Standard condition	Condition 2	Condition 3
Blast load	2.95 kg	5.9 kg	11.8 kg	47.2 kg
Thickness of blast-proof panel	25 mm	50 mm	100 mm	200 mm



7 Conclusion

With the rising incidence of terrorist attacks and installations of underground explosive facilities (e.g., ammunition magazines, hydrogen tanks, etc.) in urban areas in recent years, the risk of internal explosions is also increasing. However, most current studies on underground internal explosions examine the blast pressure through numerical analysis, while field tests are scarce. Furthermore, there is no study on the measures for reducing the acceleration propagation through the ground formation, which is the standard for deducing the safety distance at which an underground explosive facility should be located from public facilities. Therefore, in this study, the measures for reducing the propagation

of vibration propagated outward through the structure during an internal explosion by installing a blast-proof panel on the internal wall are analyzed through experiments and numerical simulation. In this study, the overall research was conducted by installing explosion-proof panels on only one wall of a structure. However, the vibration propagating to the upper part of the underground structure cannot be ignored. If the thickness of the upper ground is not sufficient, detonation or debris from the explosion may be ejected, causing great damage. Therefore, when the thickness of the upper ground is thin, it is necessary to consider installing blast-proof panels on the roof as well. Likewise, if the structure is constructed more than the second basement level, it will be

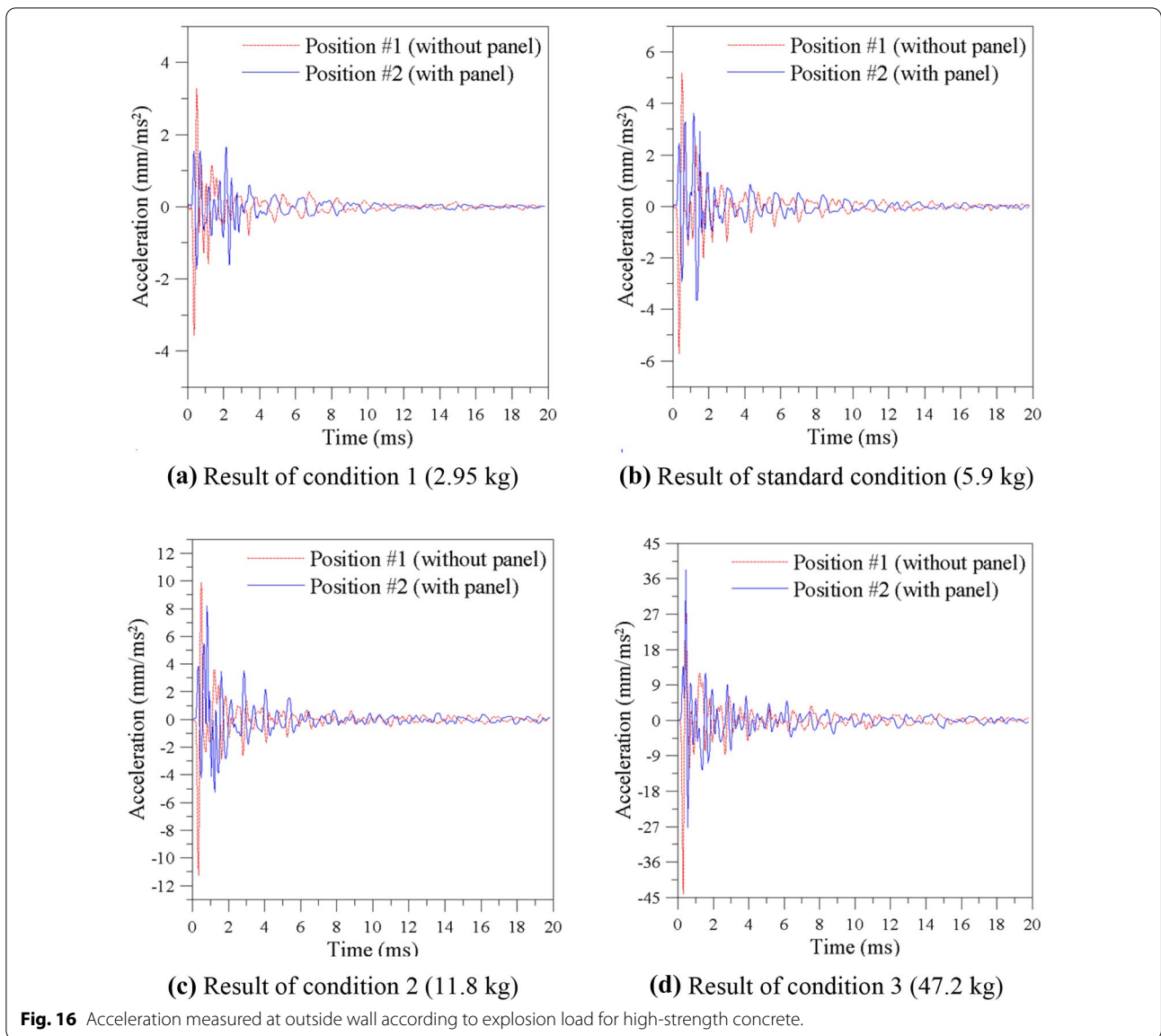


Table 8 Results of parametric study on explosion load

Blast condition (kg)	Normal strength concrete		Reduction effect (%)	High-strength concrete		Reduction effect (%)
	#1	#2		#1	#2	
2.95	4.15	2.02	51.33	3.56	1.72	51.69
5.9	6.10	4.12	32.46	5.74	3.64	36.59
11.8	12.4	9.16	26.13	11.3	8.2	27.43
47.2	37.5	33.4	10.93	44.1	38.2	13.38

possible to protect the lower level from explosion vibration by installing blast-proof panels on the floor. That is, if blast-proof panels are installed on all sides of the underground structure with the possibility of explosion,

the vibration propagating in all directions can be effectively reduced. In addition, if cultural or important facilities are located in the vicinity, a vibration reduction effect can be expected even if the panel is installed only in that

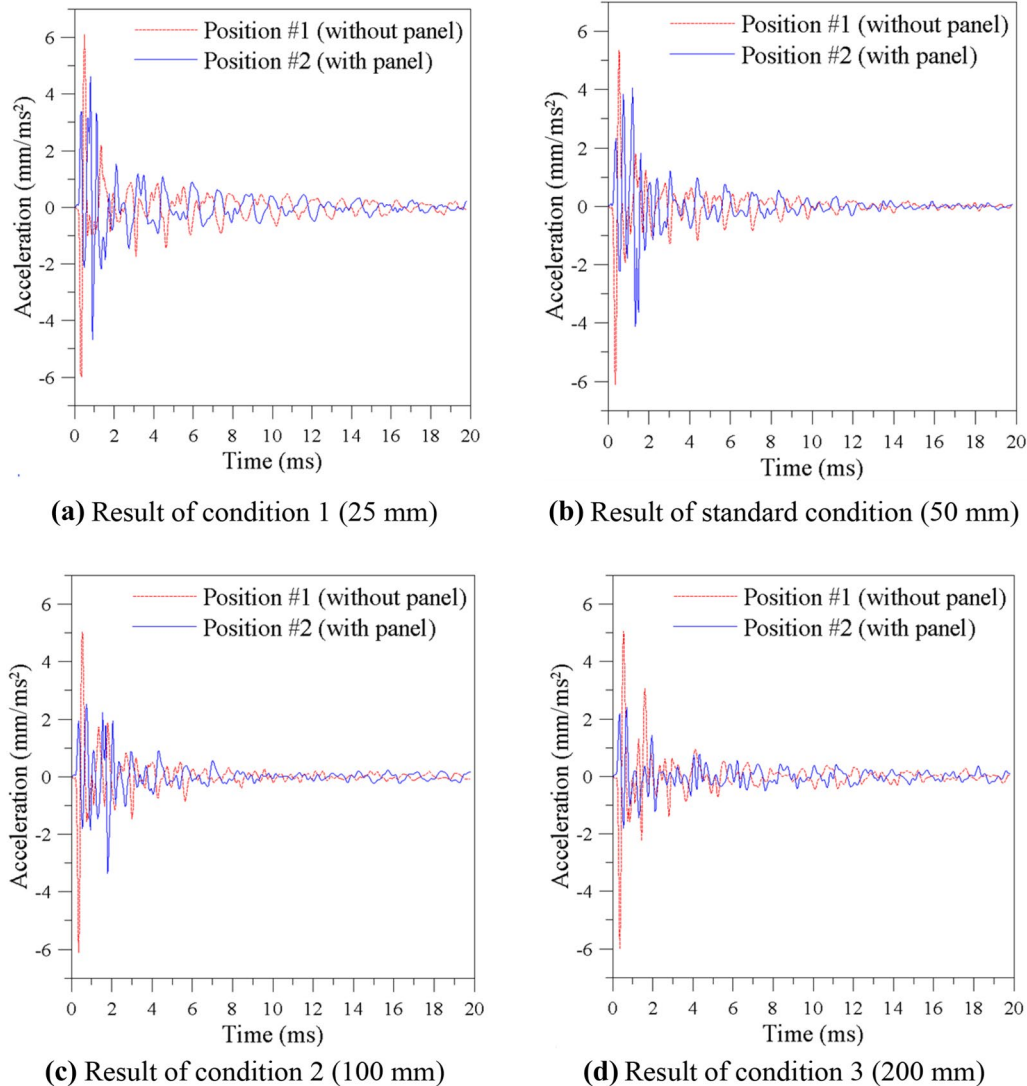


Fig. 17 Acceleration measured at outside wall according to blast-proof panel thickness for normal strength concrete.

direction for safety. The specific conclusions were as follows.

- (1) A preliminary numerical simulation was performed before the field test. The results of the preliminary numerical simulation showed that the acceleration propagated outward could be effectively reduced by installing a blast-proof panel. Particularly, the blast-proof panel effectively reduced the impact caused by the initial explosion load. In the normal strength structure, the blast-proof panel provided a smaller reduction effect of acceleration than in the high-strength structure. It can be inferred that a relatively higher displacement occurred due to
- (2) inadequate confinement and due to the large difference in material properties from the surrounding ground.
- (2) During the in situ explosion experiment, the structures could not be buried underground due to rain on the test day. Therefore, the condition was adjusted to pile the soil around the structures instead. Since the structures were not completely confined by the surrounding medium during the in situ explosion experiment, significantly larger absolute values of acceleration were measured compared to the results of the preliminary numerical simulation. Moreover, the upper slab of the normal strength structure was destroyed by the blast pres-

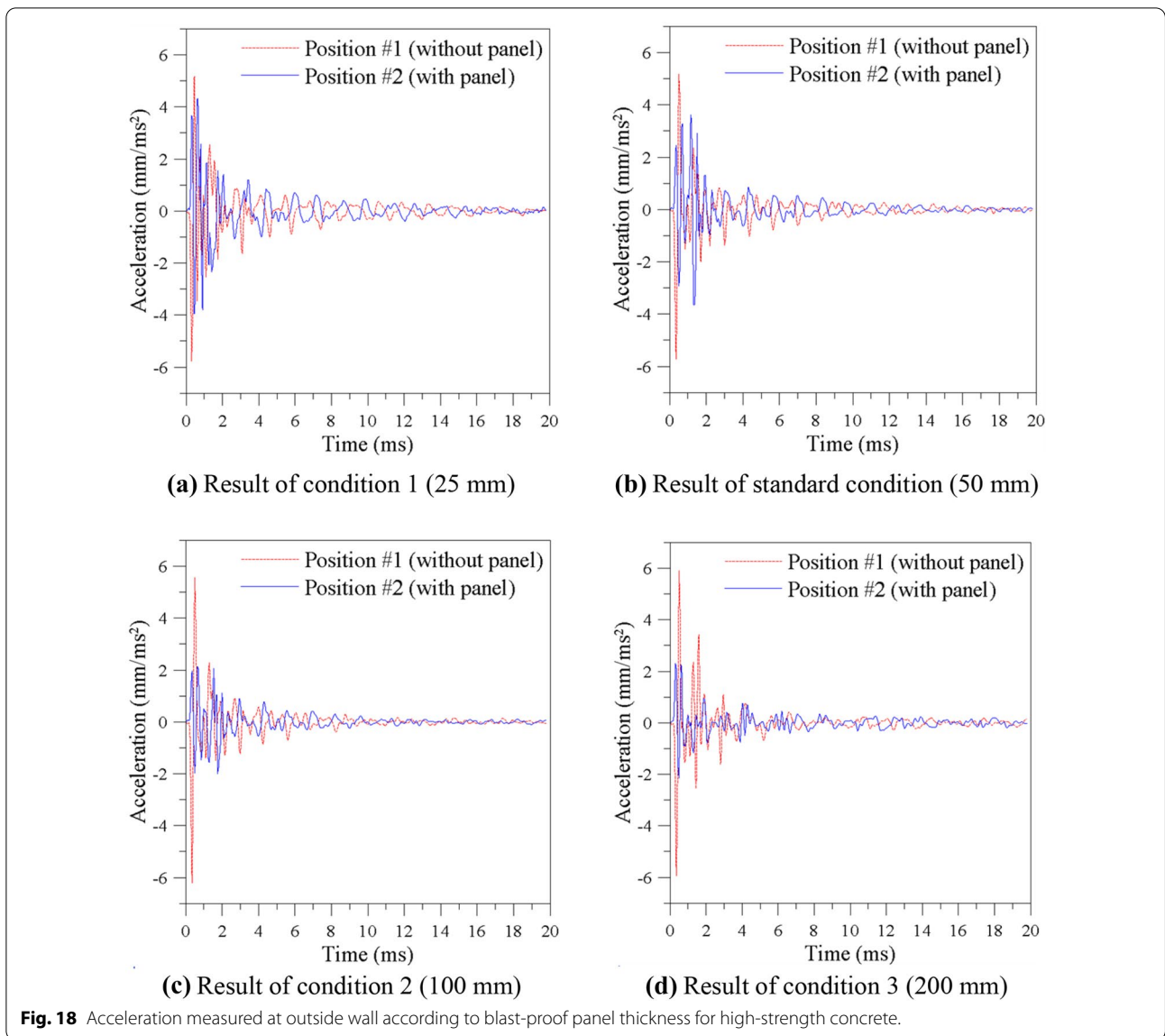


Table 9 Results of parametric study on blast-proof panel thickness

Thickness (mm)	Normal strength concrete		Reduction effect (%)	High-strength concrete		Reduction effect (%)
	#1	#2		#1	#2	
25	6.10	4.69	23.11	5.76	4.32	25.00
50	6.10	4.12	32.46	5.74	3.64	36.59
100	5.97	3.31	44.56	5.76	3.02	47.57
200	6.02	2.40	60.13	5.95	2.32	61.00

sure, which resulted in a lower vibration reduction effect of the blast-proof panel than for the high-strength structure.

- (3) Lastly, the vibration reduction effect of the blast-proof panel was evaluated according to its thickness

and the internal explosion load using the developed numerical model. The vibration transmitted through the structure itself increased as the explosion load increased, and the tremor of the materials on the side at which the panel was installed

could not be effectively prevented due to cracks in the structure. Therefore, as the explosion load increased, the reduction effect on the acceleration propagated outward by installing a blast-proof panel gradually decreased. Regarding the thickness of the blast-proof panel, the acceleration propagated outward was more effectively reduced as the thickness increased.

As the acceleration propagated outward is reduced by installing a blast-proof panel, the safety can be substantially improved, or the safe distance can be significantly decreased when constructing underground explosive facilities. A reduction in the safe distance implies that the nearby sites can be utilized for regional development, eventually leading to job creation and benefitting civil–military coexistence. Furthermore, a blast-proof panel can also be used as a fragment prevention panel or electromagnetic pulse protection material in addition to the purpose of explosion prevention.

Acknowledgements

This work was supported by research fund of the Korea Agency for Infrastructure Technology Advancement. In addition, this research was performed with the cooperation of the Steel Solution Research Lab of POSCO, Engineering school of Korea Army, and Nuclear WMD Protection Research Center; thus, the authors would like to thank them.

Authors' contributions

Each author has made substantial contributions to the Conceptualization, SP, JB, KK, and Y-JP; Investigation, SP and JB; Methodology Y-JP; Software, SP and KK; Supervision, Y-JP; Validation, SP, JB, and KK; Writing—original draft, SP; Writing—review & editing, SP and Y-JP. All authors read and approved the final manuscript.

Author's information

S.P. is an associate professor of the Department of Civil Engineering and Environmental Sciences, Korea Military Academy, Seoul 01805, Korea.

J.B. and K.K. are assistant professors of the Department of Civil Engineering and Environmental Sciences, Korea Military Academy, Seoul 01805, Korea.

Y-J.P. is a professor of the Department of Civil Engineering and Environmental Sciences, Korea Military Academy, Seoul 01805, Korea.

Funding

This work was supported by a Grant (21SCIP-B146646-04) from the Korea Agency for Infrastructure Technology Advancement.

Availability of data and materials

Some or all data, models, or code that support the findings of this study are available from the corresponding author upon reasonable request.

Declarations

Competing interests

The authors declare that they have no conflict of interest.

Received: 8 March 2021 Accepted: 4 June 2021

Published online: 21 June 2021

References

- Abbasi, T., & Abbasi, S. A. (2007). Dust explosions—Cases, causes, consequences, and control. *Journal Hazardous Materials*, *140*(1–2), 7–44. <https://doi.org/10.1016/j.jhazmat.2006.11.007>
- TM Army. (1986). Technical Manual 5–855–1; Fundamentals of Protective Design for Conventional Weapons
- Baek, J. H., Lee, H. J., & Jang, C. B. (2016). Comparison of H₂, LNG, and LPG explosion characteristics in a limited space using CFD Simulation. *Journal Korean Institute Gas*, *20*(3), 12–21.
- Cheng, Z., & Shi, Z. (2014). Vibration attenuation properties of periodic rubber concrete panels. *Construction and Building Materials*, *50*, 257–265. <https://doi.org/10.1016/j.conbuildmat.2013.09.060>
- Choi, Y., Lee, J., Yoo, Y. H., & Yun, K. J. (2016). A study on the behavior of blast proof door under blast load. *International Journal of Precision Engineering and Manufacturing*, *17*(1), 119–124. <https://doi.org/10.1007/s12541-016-0015-y>
- Choi, W. C., Yun, H. D., Cho, C. G., & Feo, L. (2014). Attempts to apply high performance fiber-reinforced cement composite (HPFRCC) to infrastructures in South Korea. *Composite Structures*, *109*, 211–223. <https://doi.org/10.1016/j.compstruct.2013.10.027>
- Department of Defense. (2017). *Manual of DOD Ammunition and Explosives Safety Standards*. Alexandria: Department of Defense Explosive Safety Board.
- Due-Hansen, M. E., & Dullum, O. (2017). Review and analysis of the explosion accident in Drevja, Norway: A consequence of fire in a mobile explosives manufacturing unit (MEMU) carrying precursors for the on-site production of bulk explosives. *Safety Science*, *96*, 33–40. <https://doi.org/10.1016/j.ssci.2017.03.003>
- Genova, B., Silvestrini, M., & Trujillo, F. L. (2008). Evaluation of the blast-wave overpressure and fragments initial velocity for a BLEVE event via empirical correlations derived by a simplified model of released energy. *Journal of Loss Prevention in the Process Industries*, *21*(1), 110–117. <https://doi.org/10.1016/j.jlp.2007.11.004>
- Golewski, G. L. (2019a). A novel specific requirements for materials used in reinforced concrete composites subjected to dynamic loads. *Composite Structures*, *223*, 110939. <https://doi.org/10.1016/j.compstruct.2019.110939>
- Golewski, G. L. (2019b). A new principles for implementation and operation of foundations for machines: A review of recent advances. *Structural Engineering and Mechanics*, *71*(3), 317–327. <https://doi.org/10.12989/sem.2019.71.3.317>
- Golewski, G. L. (2021a). On the special construction and materials conditions reducing the negative impact of vibrations on concrete structures. *Materials Today: Proceedings*, *45*(5), 4344–4348. <https://doi.org/10.1016/j.matpr.2021.01.031>
- Golewski, G. L. (2021b). The beneficial effect of the addition of fly ash on reduction of the size of microcracks in the ITZ of concrete composites under dynamic loading. *Energies*, *14*(3), 668. <https://doi.org/10.3390/en14030668>
- Homae, T., Sugiyama, Y., Wakabayashi, K., Matsumura, T., & Nakayama, Y. (2016). Water and sand for blast pressure mitigation around a subsurface magazine. *Sci. Tech. Energetic Materials*, *77*, 18–21.
- Igra, O., Falcovitz, J., Houas, L., & Jourdan, G. (2013). Review of methods to attenuate shock/blast waves. *Progress in Aerospace Sciences*, *58*, 1–35. <https://doi.org/10.1016/j.paerosci.2012.08.003>
- Jung, H., Park, S., Kim, S., & Park, C. (2017). Performance of SIFCON based HPFRCC under Field Blast Load. *Procedia Eng.*, *210*, 401–408. <https://doi.org/10.1016/j.proeng.2017.11.094>
- Kunieda, M., & Rokugo, K. (2006). Recent progress on HPFRCC in Japan required performance and applications. *Journal of Advanced Concrete Technology*, *4*(1), 19–33. <https://doi.org/10.3151/jact.4.19>
- Langdon, G. S., & Schleyer, G. K. (2005a). Inelastic deformation and failure of profiled stainless steel blast wall panels. Part I: experimental investigations. *International Journal of Impact Engineering*, *31*(4), 341–369. <https://doi.org/10.1016/j.ijimpeng.2003.12.002>
- Langdon, G. S., & Schleyer, G. K. (2005b). Inelastic deformation and failure of profiled stainless steel blast wall panels. Part II: analytical modelling considerations. *International Journal of Impact Engineering*, *31*(4), 371–399. <https://doi.org/10.1016/j.ijimpeng.2003.12.011>
- Langdon, G. S., & Schleyer, G. K. (2006). Deformation and failure of profiled stainless steel blast wall panels. Part III: Finite element simulations and

- overall summary. *International Journal of Impact Engineering*, 32(6), 988–1012. <https://doi.org/10.1016/j.ijimpeng.2004.08.002>
- Lee, J., & Choi, Y. (2018). Effects of a near-field explosion in a tunnel behind a Blast Proof Door. *International Journal of Precision Engineering and Manufacturing*, 19(4), 625–630. <https://doi.org/10.1007/s12541-018-0075-2>
- Masellis, M. (2000). Fire disaster in a motorway tunnel. *Prehospital and Disaster Medicine*, 15(S2), S74–S74. <https://doi.org/10.1017/S1049023X00031800>
- Ministry of National Defense. (2019). *Instruction of Safety Control Standard for Ammunition and Explosion*. Seoul: Ministry of National Defense.
- Moradf, R., & Groth, K. M. (2019). Hydrogen storage and delivery: Review of the state of the art technologies and risk and reliability analysis. *International Journal of Hydrogen Energy*, 44(23), 12254–12269.
- North Atlantic Treaty Organization. (2015). *Allied Ammunition Storage and Transport Publication (AASTP)-1: Nato Guidelines for the Storage of Military Ammunition and Explosives*; NATO Standardization Office. Brussels, Belgium.
- Park, S., Kim, K.-J., & Park, Y.-J. (2019). Safety evaluation method for ground ammunition and explosive storage facilities due to underground tunnel blast. *Journal of the Korea Institute of Building Construction*, 19(4), 331–339.
- Park, S., & Park, Y. J. (2020). Effect of underground-type ammunition magazine construction in respect of civil and military coexistence. *Sustainability*, 12(21), 9285. <https://doi.org/10.3390/su12219285>
- Pyo, D. Y., & Lim, O. T. (2019). A study on explosive hazardous areas in hydrogen handling facility. *Transactions of the Korean Hydrogen and New Energy Society*, 30(1), 29–34.
- Qiang, Q., Yuge, D., Shuguang, D., Hu, W., & Liangguo, H. (2020). Reliability analysis of counterweight cover-type explosion door in different periods. *Journal of Failure Analysis and Prevention*, 20(5), 1738–1753. <https://doi.org/10.1007/s11668-020-00981-z>
- Riedel, W., Kawai, N., & Kondo, K. I. (2009). Numerical assessment for impact strength measurements in concrete materials. *International Journal of Impact Engineering*, 36(2), 283–293. <https://doi.org/10.1016/j.ijimpeng.2007.12.012>
- Ruggiero, A., Bonora, N., Curiale, G., De Muro, S., Iannitti, G., Marfia, S., Sacco, E., Scafati, S., & Testa, G. (2019). Full scale experimental tests and numerical model validation of reinforced concrete slab subjected to direct contact explosion. *International Journal of Impact Engineering*. <https://doi.org/10.1016/j.ijimpeng.2019.05.023>
- Silvestrini, M., Genova, B., & Trujillo, F. L. (2009). Energy concentration factor A simple concept for the prediction of blast propagation in partially confined geometries. *Journal of Loss Prevention in the Process Industries*, 22(4), 449–454. <https://doi.org/10.1016/j.jlpi.2009.02.018>
- Sklavounos, S., & Rigas, F. (2006). Computer-aided modeling of the protective effect of explosion relief vents in tunnel structures. *Journal of Loss Prevention in the Process Industries*, 19(6), 621–629. <https://doi.org/10.1016/j.jlpi.2006.03.002>
- Sugiyama, Y., Tanaka, T., Matsuo, A., Homae, T., Wakabayashi, K., Matsumura, T., & Nakayama, Y. (2016). Numerical simulation of blast wave mitigation achieved by water inside a subsurface magazine model. *Journal of Loss Prevention in the Process Industries*, 43, 521–528. <https://doi.org/10.1016/j.jlpi.2016.07.015>
- U.S. Department of Defense. (2008). *Unified Facilities Criteria (UFC) 3–340-02 structures to resist the effects of accidental explosion*. Washington: U.S. Department of Defense.
- Uyestpruyt, D., & Monnoyer, F. (2015). A numerical study of the evolution of the blast wave shape in rectangular tunnels. *Journal of Loss Prevention in the Process Industries*, 34, 225–231. <https://doi.org/10.1016/j.jlpi.2015.03.003>
- Yoo, D. Y., Park, J. J., & Kim, S. W. (2017). Fiber pullout behavior of HPRCC: Effects of matrix strength and fiber type. *Composite Structures*, 174, 263–276. <https://doi.org/10.1016/j.compstruct.2017.04.064>
- Zhang, S., Hongtao, M. A., Huang, X., & Peng, S. (2020). Numerical simulation on methane-hydrogen explosion in gas compartment in utility tunnel. *Process Safety and Environmental Protection*, 140, 100–110.
- Zhang, Q., Qin, B., & Lin, D. C. (2013). Estimation of pressure distribution for shock wave through the junction of branch gallery. *Safety Science*, 57, 214–222. <https://doi.org/10.1016/j.ssci.2013.02.009>
- Zhang, J., & Wang, L. (2019). Personnel casualty assessment for explosion in the subway platform. *Shock and Vibration*, 2019, 1–12. <https://doi.org/10.1155/2019/8194845>
- Zhang, B., Zhao, W., Wang, W., & Zhang, X. (2014). Pressure characteristics and dynamic response of coal mine refuge chamber with underground gas explosion. *Journal of Loss Prevention in the Process Industries*, 30, 37–46. <https://doi.org/10.1016/j.jlpi.2014.03.009>
- Zheng, L., Huo, X. S., & Yuan, Y. (2008). Experimental investigation on dynamic properties of rubberized concrete. *Construction and Building Materials*, 22(5), 939–947. <https://doi.org/10.1016/j.conbuildmat.2007.03.005>

Publisher's Note

Springer Nature remains neutral with regard to jurisdictional claims in published maps and institutional affiliations.

Submit your manuscript to a SpringerOpen[®] journal and benefit from:

- Convenient online submission
- Rigorous peer review
- Open access: articles freely available online
- High visibility within the field
- Retaining the copyright to your article

Submit your next manuscript at ► [springeropen.com](https://www.springeropen.com)